

*Supplementary Information*

***Hydrochar supported bimetallic Ni-Fe alloy nanocatalysts with tailored composition, size and shape for improved biomass steam reforming performance***

Chao Gai<sup>a,b</sup>, Fang Zhang<sup>c</sup>, Tianxue Yang<sup>d</sup>, Zhengang Liu<sup>a,b\*</sup>, Wentao Jiao<sup>a,b\*</sup>, Nana Peng<sup>a,b</sup>, Tingting Liu<sup>a,b</sup>, Qianqian Lang<sup>a,b</sup>, Yu Xia<sup>a,b</sup>

**Affiliations**

<sup>a</sup>*Research Center for Eco-Environmental Sciences, Chinese Academy of Sciences, 18 Shuangqing Road, Beijing 100085, China*

<sup>b</sup>*National Engineering Laboratory for VOCs Pollution Control Material & Technology, University of Chinese Academy of Sciences, Beijing 101408, China*

<sup>c</sup>*Analytical and Testing Center, Beijing Institute of Technology, Beijing 100081, China*

<sup>d</sup>*State Key Laboratory of Environmental Criteria and Risk Assessment, Chinese Research Academy of Environmental Sciences, Beijing 100012, China*

**Figure S1.** Fabrication strategy for preparation of the hydrochar-supported, iron-incorporated nickel-based catalysts and catalytic gasification test.

**Figure S2.** N<sub>2</sub> adsorption/desorption isotherms (a) and pore-size distributions (b) of Ni<sub>0.5</sub>/HC-700, Ni<sub>0.05</sub>Fe<sub>0.05</sub>/HC-700, Ni<sub>0.25</sub>Fe<sub>0.25</sub>/HC-700 and Ni<sub>0.25</sub>Fe<sub>0.25</sub>/HC-900.

**Figure S3.** SEM images and the relative spatial distribution of elemental Ni and Fe in the fresh (A) and spent (B) catalyst of Ni<sub>0.05</sub>Ni<sub>0.05</sub>/HC-700.

**Figure S4.** Particle size distribution of the metal nanoparticles in the catalyst of Ni<sub>0.05</sub>Ni<sub>0.05</sub>/HC-700.

**Figure S5.** TEM images of the fresh (a, b) and spent (c, d) catalysts of Ni<sub>0.05</sub>Fe<sub>0.05</sub>/HC-900 and Ni<sub>0.25</sub>Fe<sub>0.25</sub>/HC-900, respectively.

**Table S1.** Surface areas, total pore volumes and average pore diameters of Ni<sub>0.5</sub>/HC-700, Ni<sub>0.05</sub>Fe<sub>0.05</sub>/HC-700, Ni<sub>0.25</sub>Fe<sub>0.25</sub>/HC-700 and Ni<sub>0.25</sub>Fe<sub>0.25</sub>/HC-900.

**Table S2.** Effect of concentrations of precursory metal salts and calcination temperature on the crystallinity indexes of the fresh and reacted catalysts.

**Table S3.** Metal loading on the monometallic and bimetallic catalysts.

**Table S4.** Carbon deposition rates for the reacted monometallic and bimetallic catalysts.

**Figure S1.** Fabrication strategy for preparation of the hydrochar-supported, iron-incorporated nickel-based catalysts and catalytic gasification test.

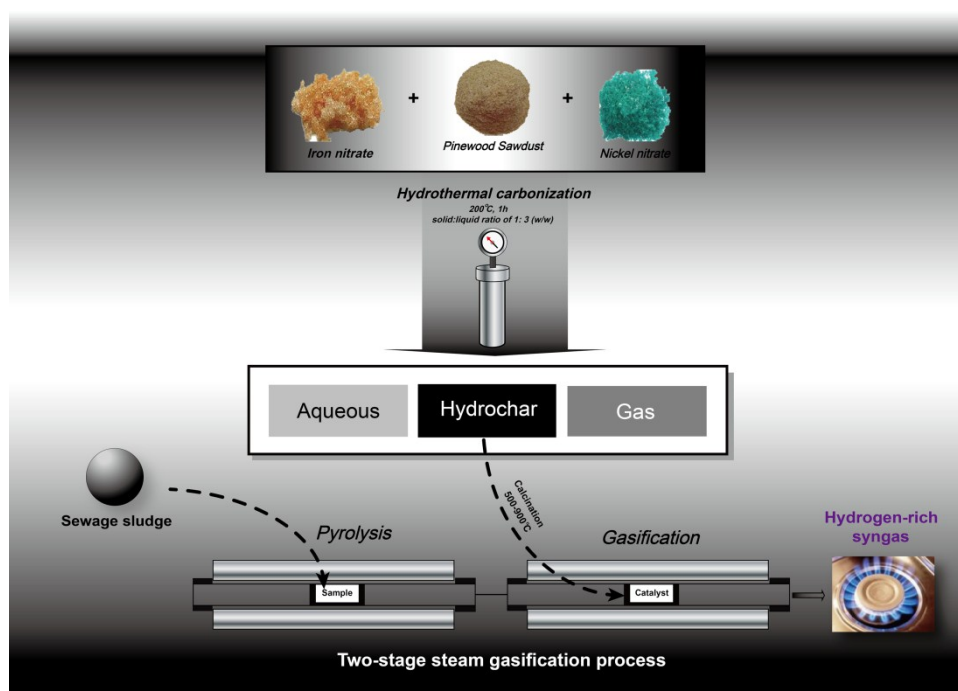


**Figure S2.** N<sub>2</sub> adsorption/desorption isotherms (a) and pore-size distributions (b) of Ni<sub>0.5</sub>/HC-700, Ni<sub>0.05</sub>Fe<sub>0.05</sub>/HC-700, Ni<sub>0.25</sub>Fe<sub>0.25</sub>/HC-700 and Ni<sub>0.25</sub>Fe<sub>0.25</sub>/HC-900.

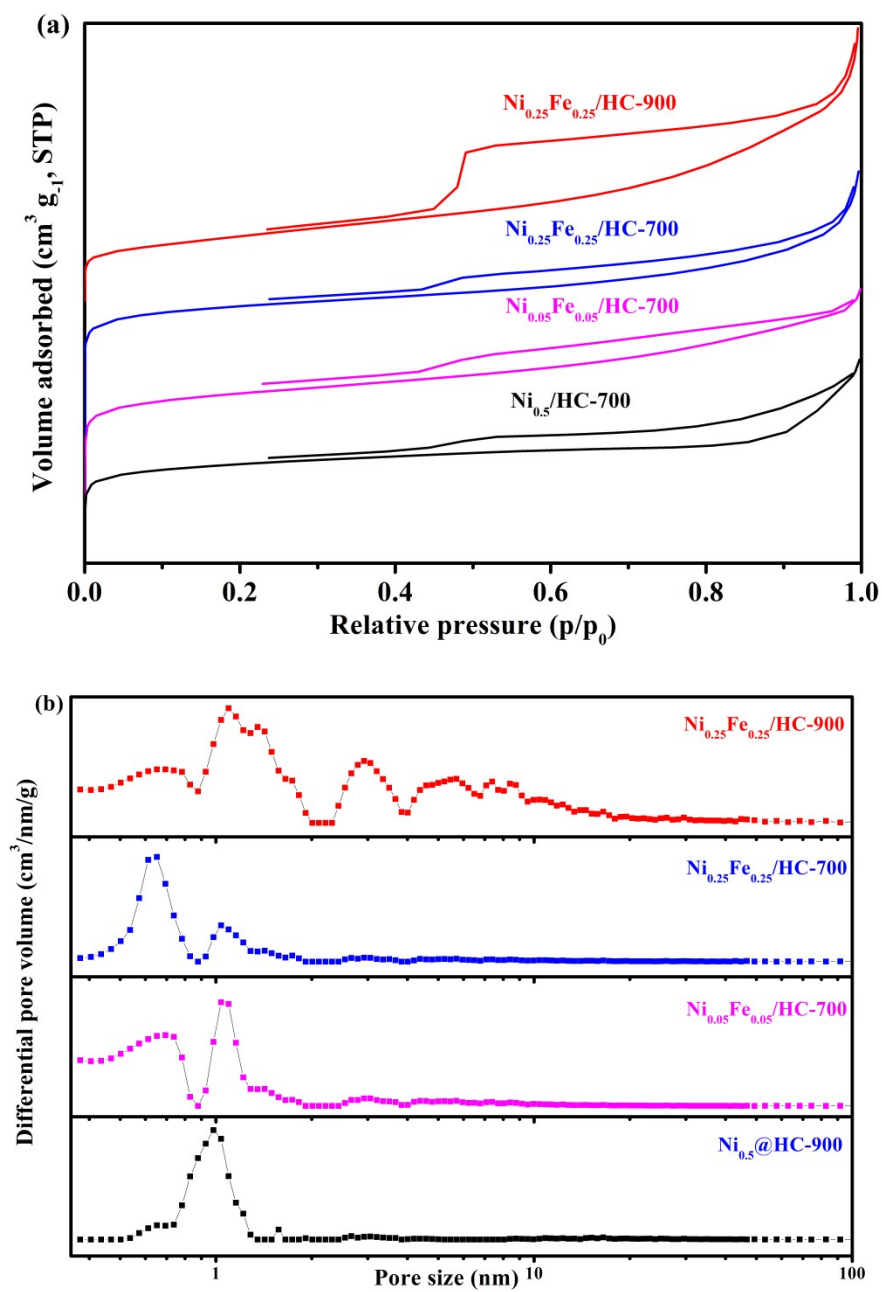


**Figure S3.** SEM images and the relative spatial distribution of elemental Ni and Fe in

the fresh (A) and spent (B) catalyst of  $\text{Ni}_{0.05}\text{Ni}_{0.05}/\text{HC-700}$ .

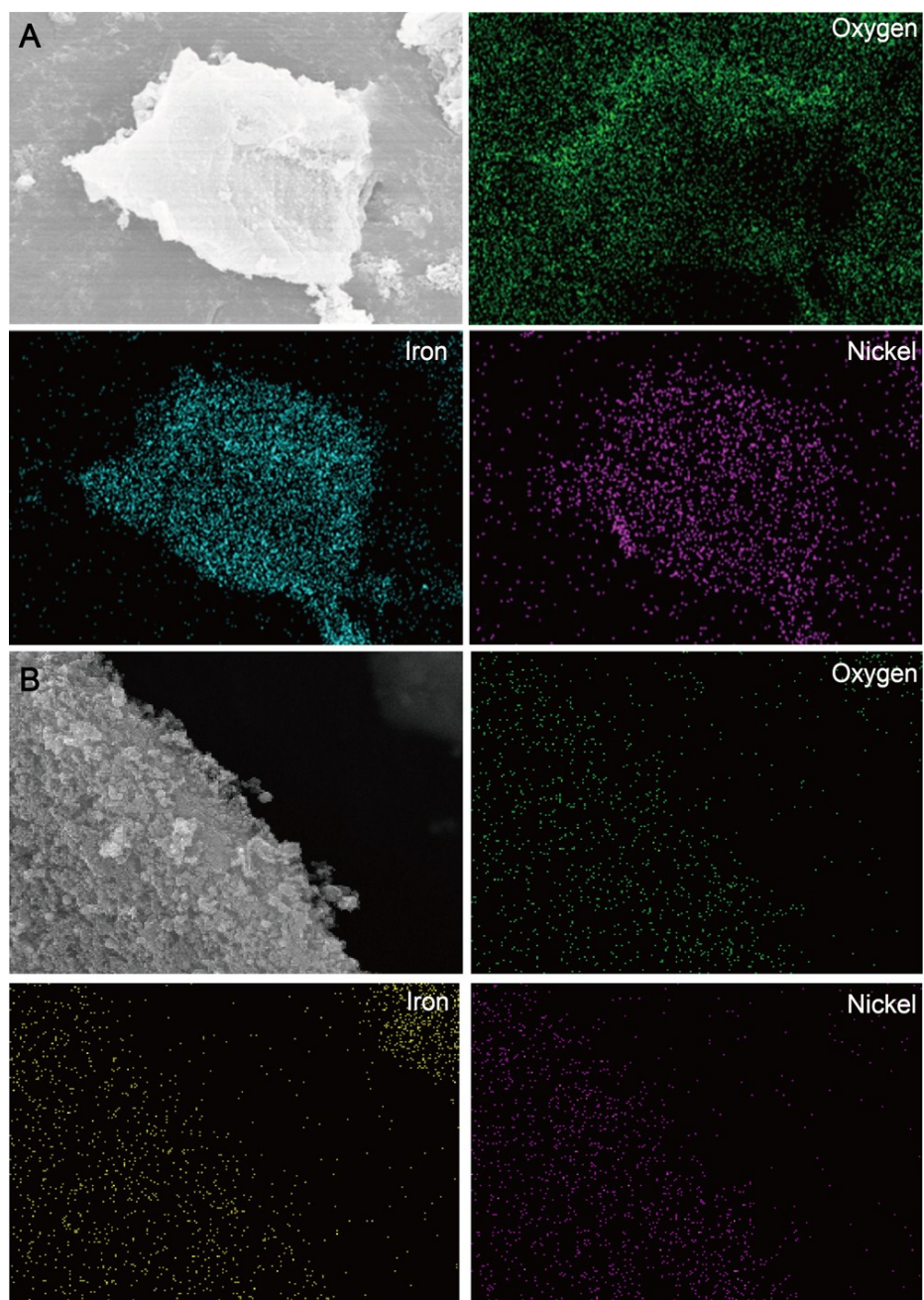


**Figure S4.** Particle size distribution of the metal nanoparticles in the catalyst of  $\text{Ni}_{0.05}\text{Ni}_{0.05}/\text{HC-700}$ .

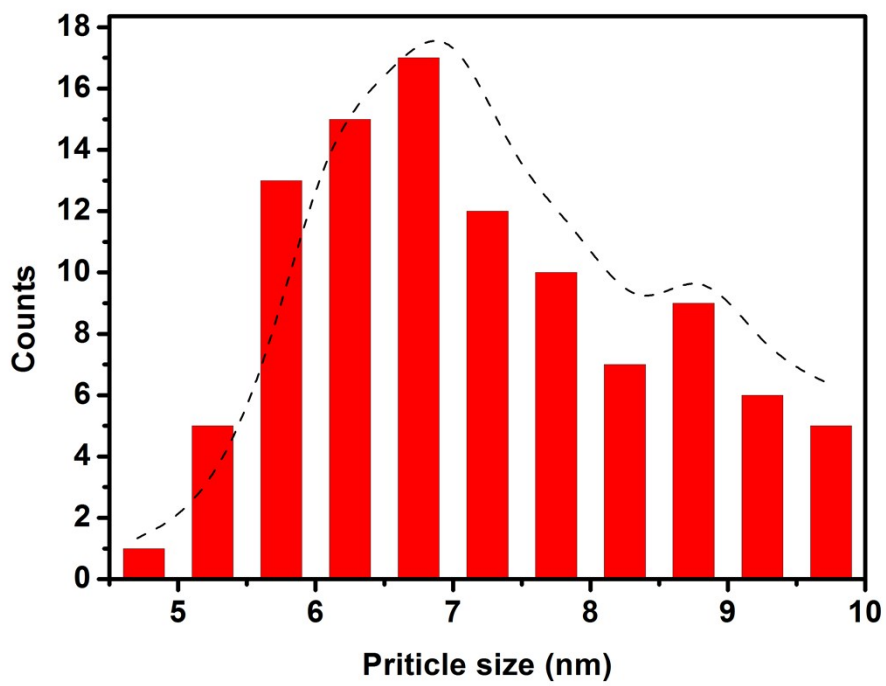


**Figure S5.** TEM images of the fresh (a, b) and spent (c, d) catalysts of

$\text{Ni}_{0.05}\text{Fe}_{0.05}/\text{HC-900}$  and  $\text{Ni}_{0.25}\text{Fe}_{0.25}/\text{HC-900}$ , respectively

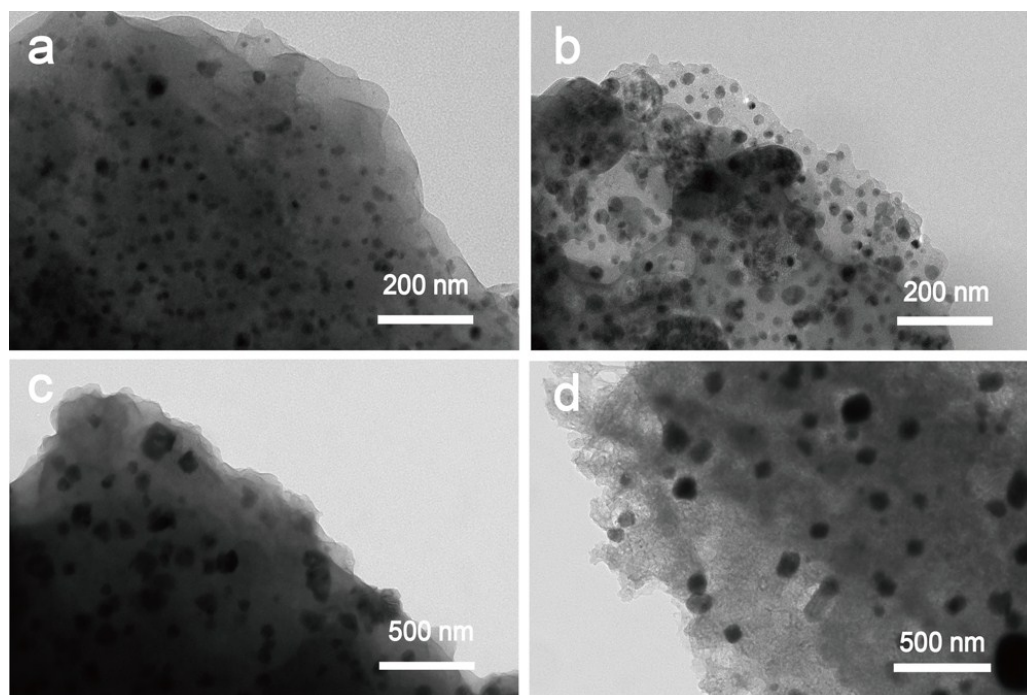


**Table S1.** Surface areas, total pore volumes and average pore diameters of Ni<sub>0.5</sub>/HC-700, Ni<sub>0.05</sub>Fe<sub>0.05</sub>/HC-700, Ni<sub>0.25</sub>Fe<sub>0.25</sub>/HC-700 and Ni<sub>0.25</sub>Fe<sub>0.25</sub>/HC-900.

Catalyst	$S_{\text{BET}}$ (m <sup>2</sup> .g <sup>-1</sup> ) 1)	$V_{\text{pore}}$ (cm <sup>3</sup> .g <sup>-1</sup> )	$AD_{\text{pore}}$ nm
Ni <sub>0.5</sub> /HC-700	320.91	0.2201	2.7432
Ni <sub>0.05</sub> Fe <sub>0.05</sub> /HC-700	373.31	0.2465	2.6411
Ni <sub>0.25</sub> Fe <sub>0.25</sub> /HC -700	323.99	0.2453	3.0289
Ni <sub>0.25</sub> Fe <sub>0.25</sub> /HC -900	147.68	0.2395	6.4874

**Table S2.** Effect of concentrations of precursory metal salts and calcination temperature on the crystallinity indexes of the fresh and reacted catalysts.

Catalyst	Temp. (°C)	CI <sub>xrd-f</sub> (%)	CI <sub>xrd-r</sub> (%)
Ni <sub>0.05</sub> Fe <sub>0.05</sub> /HC	500	6.5	8.9
	700	8.3	12.7
	900	11.9	10.6
Ni <sub>0.1</sub> /HC	500	11.2	13.5
	700	9.7	17.6
	900	12.9	9.9
Ni <sub>0.25</sub> Fe <sub>0.25</sub> /HC	500	18.2	23.5
	700	17.9	19.8
	900	16.7	10.9
Ni <sub>0.5</sub> /HC	500	12.4	14.3
	700	13.9	15.8
	900	25.2	14.7

**Table S3.** Metal loading on the monometallic and bimetallic catalysts.

Catalyst	Temp. (°C)	Ni (wt.%)	Fe (wt.%)
Ni <sub>0.05</sub> Fe <sub>0.05</sub> /HC	500	0.71	0.82
	700	0.93	1.06
	900	1.07	1.15
Ni <sub>0.1</sub> /HC	500	1.38	-
	700	1.76	-
	900	1.95	-
Ni <sub>0.25</sub> Fe <sub>0.25</sub> /HC	500	2.73	3.12
	700	3.35	3.93
	900	3.89	4.68
Ni <sub>0.5</sub> /HC	500	4.88	-
	700	6.25	-
	900	7.13	-

**Table S4.** Carbon deposition rates for the reacted monometallic and bimetallic catalysts.

Catalyst	Temp. (°C)	Rate of coke deposition (wt.%)
Ni <sub>0.05</sub> Fe <sub>0.05</sub> /HC	500	16.3
	700	13.7
	900	14.4
Ni <sub>0.1</sub> /HC	500	17.9
	700	14.2
	900	16.7
Ni <sub>0.25</sub> Fe <sub>0.25</sub> /HC	500	3.9
	700	2.8
	900	3.1
Ni <sub>0.5</sub> /HC	500	5.3
	700	3.2
	900	4.7

<sup>a</sup>Reaction conditions: reaction temperature: 500-900 °C; steam flow rate: 0.05 g min<sup>-1</sup>;  
reaction time: 0.5 h; mass of catalyst: 300 mg.